JAERI-M
86-154

CHARACTERISTICS OF GAS STRIPPER CELL FOR PRODUCTION OF MULTI-CHARGED IONS

October 1986

Masao SATAKA and Kiyoshi KAWATSURA

日本原子力研究所
Japan Atomic Energy Research Institute

JAERI-Mレポートは，日本原子力研究所が不定期に公刊している研究報告書です。
入手の問合わせは，日本原子力研究所技術情報部情報資料課（〒319-11 茨城県那珂郡東海村）あて，お申しこしください。なお，このほかに財団法人原子力弘済会資料センター（〒319 11 茨城県那珂郡東海村日本原子力研究所内）で複写による実費領布をおこなっております。

JAERI-M reports are issued irregularly.
Inquiries about availability of the reports should be addressed to Information Division Department of Technical Information, Japan Atomic Energy Research Institute, Tokaimura, Naka-gun, Ibaraki-ken 319-11, Japan.

編集兼発行　日本原子力研究所
印　　刷　日青工業株式会社

JAERI-M 86-154

CHARACTERISTICS OF GAS STRIPPER CELL FOR PRODUCTION OF MULTI-CHARGED IONS

Masao SATAKA and Kiyoshi KAWATSURA

Department of Physics, Tokai Research Establishment
Japan Atomic Energy Research Institute
Tokai-mura, Naka-gun, Ibaraki-ken

(Received October 2, 1986)

A gas stripper cell has been constructed in order to investigate collision processes of multi-charged ions incident on atoms and molecules in a few MeV energy region. This apparatus consists of two parts, namely the gas cell and the charge selector. The design principles as well as the characteristics of the constituent components are described. Experimental results show that this apparatus works well as we have expected.

Keywords: Gas Stripper Cell, Construction, Multi-charged Ion, MeV Range

JAERI －M 86－154

多価イオン生成のためのガス・ストリッパーセルの試作

日本原子力研究所東海研究所物理部
左高　正雄・川面　　澄

（ 1986 年 10 月 2 日受理 ）

エネルギー領域数ＭｅＶでの多価イオンと原子分子の衝突過程を研究するためにガスストリッパーセルを製作した。この装置はバンデグラフ加速器からの一価イオンを多価イオンに変換するもので，ガスセルと電荷分析器の２つの部分から成り立っている。各部分の設計方針と出来上がった装置の性能が本文で述べられる。また本装置を用いて，ヘリウムの平衡電荷分布が測定され，その結果から本装置が設計通り稼動していることが示される。

東海研究所：〒319－11　茨城県那珂郡東海村白方白根２－４

CONTENTS

目　　次

1. INTRODUCTION

Collision processes of multi-charged ion impact on atoms and molecules are of importance not only in atomic physics but in plasma physics and in laser physics. Nevertheless, studies on these processes have been performed in past a few years, because of difficulties in production of the multi-charged ions.

An experimental apparatus for production of multi-charged ions has been constructed at 2 MV Van de Graaff facility of JAERI (2 MV VdG), applying to charge stripping processes of energetic ion beams. This apparatus is aimed to produce the data for the atomic and molecular processes in fusion research. The ion beams produced by this apparatus will be used to the following measurements: (1) the measurements of charge changing cross sections of multi-charged ions, (2) the measurements of energy and angular spectrum of X-rays and electrons from atoms and molecules by multi-charged ion impacts, (3) the measurements of recoil ions produced by multi-charged ion impacts on atoms and molecules.

In general, the multi-charged ions are obtained by extraction from multiply charged ion sources[1] (for example EBIS, ECR ion source, laser ion source etc.) or by charge-stripping of singly charged ions. It is difficult to mount a multiply charged ion source at the high voltage terminal of 2 MV VdG. In high energy region, ions are effectively charge-stripped in the collision with gas and solid targets. We have

selected the charge-stripping method because of simplicity of the equipment.

we had preliminarily measured the equilibrium charge distribution of carbon ions after passing through both gas and foil stripper.[2] the mean charge state of foil-stripped ions was higher than that of gas-stripped ion. The thickness of the foil was about 15 $\mu g/cm^2$. But, in the energy region of a few MeV, the foil-stripped ions were spatially spread by interaction with foils, but the gas-stripped ions were not practically spread. Then the effective intensities of multi-charged ions stripped by gas were higher than these by foils. Then we chose the gas stripper for production of multi-charged ions.

Referring to Fig. 1.1, we shall state the general principle of the operation of the apparatus. The singly charged ions produced in the ion source are extracted, accelerated by 2 MV VdG and, after energy analyzed, introduced in this apparatus. The apparatus consists of two main parts, namely the gas cell (G) and the charge selector (D), each of which is differentially pumped with independent diffusion pump systems. In the gas cell, the ions are charge-stripped by collision of gas atoms. The ions emerged from the gas cell have several charge states. These ions are magnetically selected with ionic charge by charge selector. Then multi-charged ions with definite charge are obtained. A photograph of the apparatus is shown in Fig. 1.2.

The design principle is that no charge exchange process significantly contributes to the magnetically selected ion

beam and no beam attenuation effect significantly contribute to 2 MV VdG beam transport system, even when the gas is fed to the gas cell at sufficient pressure to maximum efficiency for production of multi-charged ions.

In Sec. 2.1 of this paper we describe the design and operation of the gas cell and pumping system, while in Sec. 2.2 a detailed discussion is given for the design of analyzing magnet.

2. APPARATUS

2.1 GAS CELL AND PUMPING SYSTEM

2.1.1 REQUIREMENTS

For the purpose of this apparatus, the following conditions are required:

1) The gas pressure in the gas cell is required to be higher than 1×10^{-1} Torr.
2) The pressure outside of the gas cell is required to be 1×10^{-4} Torr.
3) The inlet and outlet of the gas cell is must be greater than 2 mm diameter not to disturb the ion beam.
4) The pressure of the chamber where the charge-selected beams are introduced is required to be less than 1×10^{-7} Torr.

2.1.2 CONDUCTANCE AND PUMPING SPEED

First, we must decide the conductance C of the path which ion beam pass through, for design of gas cell and pumping speed.

Throughput Q of molecular flow, across which a pressure difference P_1-P_2 exists, is given by

$$Q = C\,(P_2 - P_1). \tag{2.1}$$

Throughput Q is also given by

$$Q = P\,S + V\frac{dP}{dt} \tag{2.2}$$

in terms of pressure P, speed of evacuation S, volume of vacuum vessel V and time t.[3] In steady state, $\frac{dP}{dt} = 0$, the equation (2.2) yields

$$Q = P\,S. \tag{2.3}$$

Hence, equations (2.1) and (2.3) yield,

$$P_1\,S = C\,(\,P_2 - P_1\,) \tag{2.4}$$

$$S = C\,(\,\frac{P_2}{P_1} - 1\,). \tag{2.5}$$

Now, as P_2/P_1 should be greater than 10^3, equation (2.5) yields

$$\frac{P_2}{P_1} = \frac{S}{C}\,. \tag{2.6}$$

Then, in this case of $P_2/P_1 >> 1$, the pressure ratio is given by the ratio S to C.

2.1.3 PUMPING SYSTEM

As the throughput Q to the gas cell is large, it is important to correctly decide parameters of the vacuum pump system. We adopted the 6" oil diffusion pump with cold trap for main pump.

A pumping speed, ultimate vacuum, maximum throughput and ultimate forepressure of the diffusion pump was 1200 ℓ/sec, 1×10^{-8} Torr, 2 Torr ℓ/sec and 0.65 Torr, respectively. In Fig. 2.1 shown is a Q-P diagram. Curve DP shows inlet pressure as a function of throughput Q. Curve $(DP)_B$ shows a maximum forepressure. Curve $(DP)_B$ is approximated to straight line. From the diagram, throughput of 0.6 Torr ℓ/sec is obtained using the forepump with pumping speed of 10 ℓ/sec. We used the rotary pump with a performance which is shown by curve RP in Fig. 2.1. Using the rotary pump the maximum throughput of diffusion pump can be attained. It is needed to prevent the contamination by backstreaming to the work

chambers. All the diffusion pump systems are equipped with water-cooled baffles. Especially, diffusion pump systems B and C are equipped with liquid N_2 cold traps, as charge states of ions emerged from gas cell may not change by collision of hydrocarbon molecules. The effective pumping speeds should be fairly decreased for both pump system.

2.1.4 DESIGN OF GAS CELL

The gas cell must be filled sufficient target gas atoms to reach the charge-equilibrium thickness of fast ion beam. As the results of preliminary experiment,[2] the target thickness should be thicker than $1x10^{14}$ atom/cm^2. If the length of gas cell is 30 cm, the gas cell pressure is about $1x10^{-1}$ Torr. As pressure of beam duct of the accelerator system is about $1x10^{-7}$ Torr, the gas cell must be differentially pumped. The pressure outside of the gas cell is decided by the conductances of beam inlet and exit of the gas cell and the pumping speeds of differential pumping systems. The effective pumping speed of the pumping system A is 480 ℓ/sec. The effective pumping speeds of the pumping systems B and C are 280 ℓ/sec. These values are included conductances of a cold trap, a gate valve and a vacuum piping. In the pumping system B, we assume $P_G/P_B=10^3$, then conductance C_{BG} between the chamber (B) and the gas cell (G) is given by equation (2.6) as follows:

$$C_{BG} = 280/10^3 = 0.28 \ (\ell/\text{sec}).$$

If the beam exit is assumed to be an aperture, diameter of the aperture is 1.6^{ϕ}. Since the diameter of ion beam from

accelerator is about 3^{ϕ}, the ion beam is cut off by the aperture. Making the beam inlet and exit in conduit tube, the inner diameters of these can be enlarged as the same conductance C_{BG}. The conductance of conduit tube is given by

$$C = 97.1 \frac{a^3}{\ell + \frac{8a}{3}} \quad (\ell/\text{sec}) \qquad (2.7)$$

where

a: radius of tube (cm)

ℓ: length of tube (cm)

In table 2.1 the conductance of conduit tube is tabulated. From the Table 2.1, proper dimension for this apparatus is found as:

ℓ = 50 mm

a = 2.5 mm

2.1.5 MANUFACTURING OF VACUUM SYSTEM

In Fig. 2.2 shown is the pumping system. The main part of the vacuum system is made of type 304 stainless steel and sealed with use of viton O-rings and copper gaskets. The base pressure 2×10^{-5} Torr in the gas cell, 1.5×10^{-7} Torr in the chamber (A), 4×10^{-8} Torr in the chamber (B) and 2×10^{-8} Torr in the chamber (C) can be easily attained. The gas effused from the gas cell is pumped by 6" diffusion pump systems attached to the chamber (A) and the chamber (B). The chamber (A) and the chamber (B) are separated from gas cell by a 5 mm diameter and 50 mm long conduit tubes. The analyzing tube in the analyzing magnet (D) is differentially pumped by 6" diffusion pump systems B and C. In Fig. 2.3 shown is the gas

pressures of chambers (A), (B) and (C) as a function of gas pressure in the gas cell. From the figure, it is found that the pressure differential of 10^3 was obtained between gas cell and both chambers (A) and (B). Therefore, no charge exchange processes significantly contribute to magnetically selected multi-charged ions. The total vacuum system is designed to keep a clean vacuum for the whole system except for around the chamber (A).

2.2 CHARGE SELECTOR

2.2.1 REQUIREMENTS

1) The resolution; $\Delta m/m = 0.1$ was aimed at in this analyzer.
2) The largest transmission possible, making compromise with the resolution, is required.
3) The mass energy product of the magnet must be 18 MeV amu same as the magnet equipped at 2 MV VdG accelerator of JAERI

2.2.2 ION OPTICS OF MAGNET

The ion orbit is shown in Fig. 2.4. Magnetic field is enclosed two plates between y'P and y"P intersecting at the angle Φ and extending perpendicularly to the plane of the drawing. If an ion beam is injected into a point O' at the right angle through trajectory x'O', after traveling through a magnetic field along circular arc of radius a, the beam is ejected from a point O" at right angle. The trajectory x'O'O"x" is named a central orbit. The image formation is discussed based on the axis of co-ordinate x'O'O"x".

Ion beam is emitted from a point A'(ℓ',b) which is situated near the central orbit in the field free space. The beam is injected into a magnetic field at angle α' to the normal n'. The beam travels through the field along circular arcs of the radius r and the beam leaves from the field at angle α'' to the normal n". The beam is focused in a point A"(ℓ'',b"). Where, position A' and A" are represented by the (x',y') co-ordinate and (x",y") co-ordinate, respectively.

Then, conditions of the image formation are given by the following equations,[4)]

$$(\ell' - g)(\ell'' - g) = f^2 \tag{2.8}$$

or

$$\frac{1}{\ell' - h} + \frac{1}{\ell'' - h} = \frac{1}{f} \tag{2.9}$$

where

$$g = a \cot \Phi \tag{2.10}$$

$$h = - a \tan (\Phi/2) \tag{2.11}$$

$$f = \frac{a}{\sin \Phi}. \tag{2.12}$$

If equation (2.8) or (2.9) is satisfied, the y" co-ordinate of the image point A", b" is given by

$$b'' = (\beta + \gamma)\, a \left(1 + \frac{f}{\ell' - g} \right) - b' \left(\frac{f}{\ell' - g} \right) \tag{2.13}$$

where

$$v = v_0 (1 + \beta)$$

$$m = m_0 (1 + \gamma).$$

The image multiplication rate G and the dispersion coefficient K are defined by

$$G = \left(\frac{|b''|}{|b'|} \right)_{\beta=0} = \frac{f}{\ell' - g} \tag{2.14}$$

$$K = a \left(1 + \frac{f}{\ell' - g} \right). \qquad (2.15)$$

On the right hand side of equation (2.13), the term corresponds to the mass dispersion and the second term corresponds to energy dispersion. Then, the mass dispersion and the energy dispersion are defined respectively by

$$D = (\beta + \gamma)\, a \left(1 + \frac{f}{\ell' - g} \right) \qquad (2.16)$$

$$d = \beta\, a \left(1 + \frac{f}{\ell' - g} \right). \qquad (2.17)$$

Let the width of the incident slit S, in the case of parallel beam, the mass resolution R is defined as follows;

$$R = \frac{m}{\Delta m} = \frac{1}{\frac{2SG}{K} + \frac{\Delta V}{V}}$$

$$= \frac{a}{S + a \frac{\Delta V}{V}}. \qquad (2.18)$$

2.2.3 RELATION BETWEEN V_a (ACCELERATION POTENTIAL OF ION) AND H (MAGNETIC FLUX DENSITY IN THE MAGNET)

$$V_a = 4.28 \times 10^{-5} \frac{a^2 H^2}{\frac{m}{e}} \qquad (2.19)$$

or

$$H = 6.94 \times 10^{-3} \frac{1}{a} \left(\frac{m}{e} V_a \right)^{\frac{1}{2}}. \qquad (2.20)$$

m ; the mass expressed in atomic mass units

e ; the charge expressed in number of electronic charges on the ions

V_a; acceleration potential of ions in units of electron volt

H ; magnetic flux density in the magnet expressed in units of Gauss.

2.2.4 DESIGN PRINCIPLE AND EXPECTED CHARACTERISTICS

The characteristics of the manufactured magnet is tabulated in Table 2.2. Taking account of allowances of the target room, we chose a small magnet. But, as mentioned in Sec. 2.3.1, mass-energy product must be 18 MeV amu. And it should be expected that the magnetic flux density is less than 10 k Gauss. Since the maximum acceleration potential is 1.8 MeV, the radius of central orbit a is given using equation (2.19)

a = 650 mm.

A diffraction angle is decided to be 20°, then the width of magnetic pole becomes to be about 70 mm. By equation (2.12), the focus length f is calculated to be 1900 mm.

Table 2.2 Performance of analyzing magnet

Radius of central orbit	650 mm
Diflection angle	20°
Gap of magnetic pole	15 mm
Width of magnetic pole	70 mm
Maximum magnetic flux density	10 kG
Mass-energy product	18 MeV amu

As ion beam from 2 MV VdG is shaped at most 3 mm diameter by the conduit tube equipped at the gas cell, the

gap of pole piece is sufficient for the ion beam to pass through.

Fig. 2.5 shows the calibration curve of the magnetic flux density of the magnet to the electric current through the magnetic coil. Figs. 2.6 and 2.7 show the magnetic field distribution parallel and perpendicular to the ion beam direction, respectively. The effect of fringing magnetic field to the focus point has been corrected by the method of so called "gap width correction".

Since the ion beam is regarded as a parallel beam, the cross section of ion beam shaped in circle. The resolution R is calculated from equation (2.18)

$$R = 650/5 = 130.$$

The resolution is sufficient to the purpose of charge selector.

3. EXAMPLES OF APPLICATIONS

Using the gas stripper cell described in this paper, we have performed the measurement of charge state distribution of helium passing through the argon gas as a function of target pressure in the energy region between 0.3 and 1.5 MeV. Ion beams were introduced to gas cell in which the ion beams were charge-changed by argon and then charge state selected by the magnet. The target pressure was measured by means of a Schulz gauge and an ionization gauge. The current of ion beam components was measured by a Faraday cup. The neutral beam component was also measured by the Faraday cup, which was used to measure the secondary electrons ejected by He^0 beam impact onto the cup. the detection efficiencies of neutral beam were measured before and after the each measurement. Typical beam current of incoming He^+ beam was about 60 nA.

In Fig. 3.1 shown are the pressure dependencies of the fractions of outgoing He^0, He^+ and He^{2+} beams (F_i) normalized by intensities of the outgoing ion beams at beam energy of 1.0 MeV. The figure shows that equilibrium charge by argon gas is attained at the pressure higher than 10^{-1} Torr.

In Fig. 3.2 shown are the pressure dependencies of the fractions of outgoing He^0, He^+ and He^{2+} beams (F'_i) normalized by intensities of the incident ion beams at beam energy of 1.0 MeV. The figure shows that the maximum values of F'_0 and F'_2 is not identical with the equilibrium value. F'_0 and F'_2 is highest at the gas cell pressure of about 5×10^{-1} Torr. This pattern may be caused by increase of

angular spreading of scattered helium with the target gas atoms.

In Fig. 3.3 shown are the equilibrium charge state fractions of He^0, He^+ and He^{2+} beams, $F_{0\infty}$, $F_{1\infty}$ and $F_{2\infty}$, respectively, in argon gas with the data measured by Snitzel[5] and Allison[6] for comparison. The measured equilibrium charge state fraction is in good agreement with the data of Snitzer where they overlap at 0.3 MeV. It is seen in the Fig. 3.3 that the data measured by Allison, by Snitzer and by present authors is consistently connected over the energy region higher than 10 keV.

It is found that F_2 is increased with increasing incident energy and at the energy higher than 1.0 MeV, more than 80 % of He^+ beam is converted to He^{2+} by this apparatus. At the minimum energy of 0.3 MeV, F_2 is about 10 %, then He^{2+} beam is applicable to atomic collision experiment.

4. CONCLUSION

The performance of the experimental apparatus has been carefully examined. The apparatus constructed works well as expected by the design. With use of this apparatus, we intend to investigate atomic collision processes taking part in multi-charged ions.

REFERENCES

1) D. J. Clark, IEEE Trans. Nucl. Sci., NS-23, 1166 (1976).

2) private communication.

3) A. Roth, "Vacuum Technology", (North-Holland, Amsterdam, 1976) pp. 65.

4) R. Herzog, Z. Physik, 89, 447 (1934).

5) E. Snitzer, Phys. Rev., 89, 1237 (1953).

6) S. A. Allison, Rev. Mod. Phys., 30, 1137 (1958).

Table 2.1 The conductance of conduit tube with circular cross section (ℓ/sec)

RADIUS	LENGTH (MM)										
(MM)	0.0	10.0	20.0	30.0	40.0	50.0	60.0	70.0	80.0	90.0	100.0
0.50	9.10E-02	1.07E-02	5.69E-03	3.87E-03	2.94E-03	2.36E-03	1.98E-03	1.70E-03	1.49E-03	1.33E-03	1.20E-03
1.00	3.64E-01	7.67E-02	4.28E-02	2.97E-02	2.28E-02	1.84E-02	1.55E-02	1.34E-02	1.17E-02	1.05E-02	9.46E-03
1.50	8.19E-01	2.34E-01	1.37E-01	9.64E-02	7.45E-02	6.07E-02	5.12E-02	4.43E-02	3.90E-02	3.49E-02	3.15E-02
2.00	1.46E+00	5.07E-01	3.07E-01	2.20E-01	1.71E-01	1.40E-01	1.19E-01	1.03E-01	9.10E-02	8.15E-02	7.37E-02
2.50	2.27E+00	9.10E-01	5.69E-01	4.14E-01	3.25E-01	2.68E-01	2.28E-01	1.98E-01	1.75E-01	1.57E-01	1.42E-01
3.00	3.28E+00	1.46E+00	9.36E-01	6.90E-01	5.46E-01	4.52E-01	3.86E-01	3.36E-01	2.98E-01	2.68E-01	2.43E-01
3.50	4.46E+00	2.15E+00	1.42E+00	1.06E+00	8.44E-01	7.02E-01	6.00E-01	5.25E-01	4.66E-01	4.19E-01	3.81E-01
4.00	5.82E+00	3.01E+00	2.03E+00	1.53E+00	1.23E+00	1.02E+00	8.79E-01	7.70E-01	6.85E-01	6.17E-01	5.62E-01
4.50	7.37E+00	4.02E+00	2.77E+00	2.11E+00	1.70E+00	1.43E+00	1.23E+00	1.08E+00	9.62E-01	8.67E-01	7.90E-01
5.00	9.10E+00	5.20E+00	3.64E+00	2.80E+00	2.28E+00	1.92E+00	1.66E+00	1.46E+00	1.30E+00	1.17E+00	1.07E+00
5.50	1.10E+01	6.55E+00	4.66E+00	3.62E+00	2.96E+00	2.50E+00	2.16E+00	1.91E+00	1.71E+00	1.54E+00	1.41E+00
6.00	1.31E+01	8.07E+00	5.83E+00	4.56E+00	3.75E+00	3.18E+00	2.76E+00	2.44E+00	2.18E+00	1.98E+00	1.81E+00
6.50	1.54E+01	9.76E+00	7.14E+00	5.63E+00	4.65E+00	3.96E+00	3.45E+00	3.05E+00	2.74E+00	2.48E+00	2.27E+00
7.00	1.78E+01	1.16E+01	8.61E+00	6.84E+00	5.68E+00	4.85E+00	4.23E+00	3.76E+00	3.38E+00	3.06E+00	2.81E+00
7.50	2.05E+01	1.37E+01	1.02E+01	8.19E+00	6.83E+00	5.85E+00	5.12E+00	4.55E+00	4.10E+00	3.72E+00	3.41E+00
8.00	2.33E+01	1.59E+01	1.20E+01	9.68E+00	8.11E+00	6.97E+00	6.11E+00	5.44E+00	4.91E+00	4.47E+00	4.10E+00
8.50	2.63E+01	1.83E+01	1.40E+01	1.13E+01	9.52E+00	8.21E+00	7.21E+00	6.44E+00	5.81E+00	5.29E+00	4.86E+00
9.00	2.95E+01	2.08E+01	1.61E+01	1.31E+01	1.11E+01	9.57E+00	8.43E+00	7.53E+00	6.81E+00	6.21E+00	5.71E+00
9.50	3.29E+01	2.36E+01	1.84E+01	1.50E+01	1.27E+01	1.11E+01	9.76E+00	8.73E+00	7.90E+00	7.22E+00	6.64E+00
10.00	3.64E+01	2.65E+01	2.08E+01	1.71E+01	1.46E+01	1.27E+01	1.12E+01	1.00E+01	9.10E+00	8.32E+00	7.67E+00

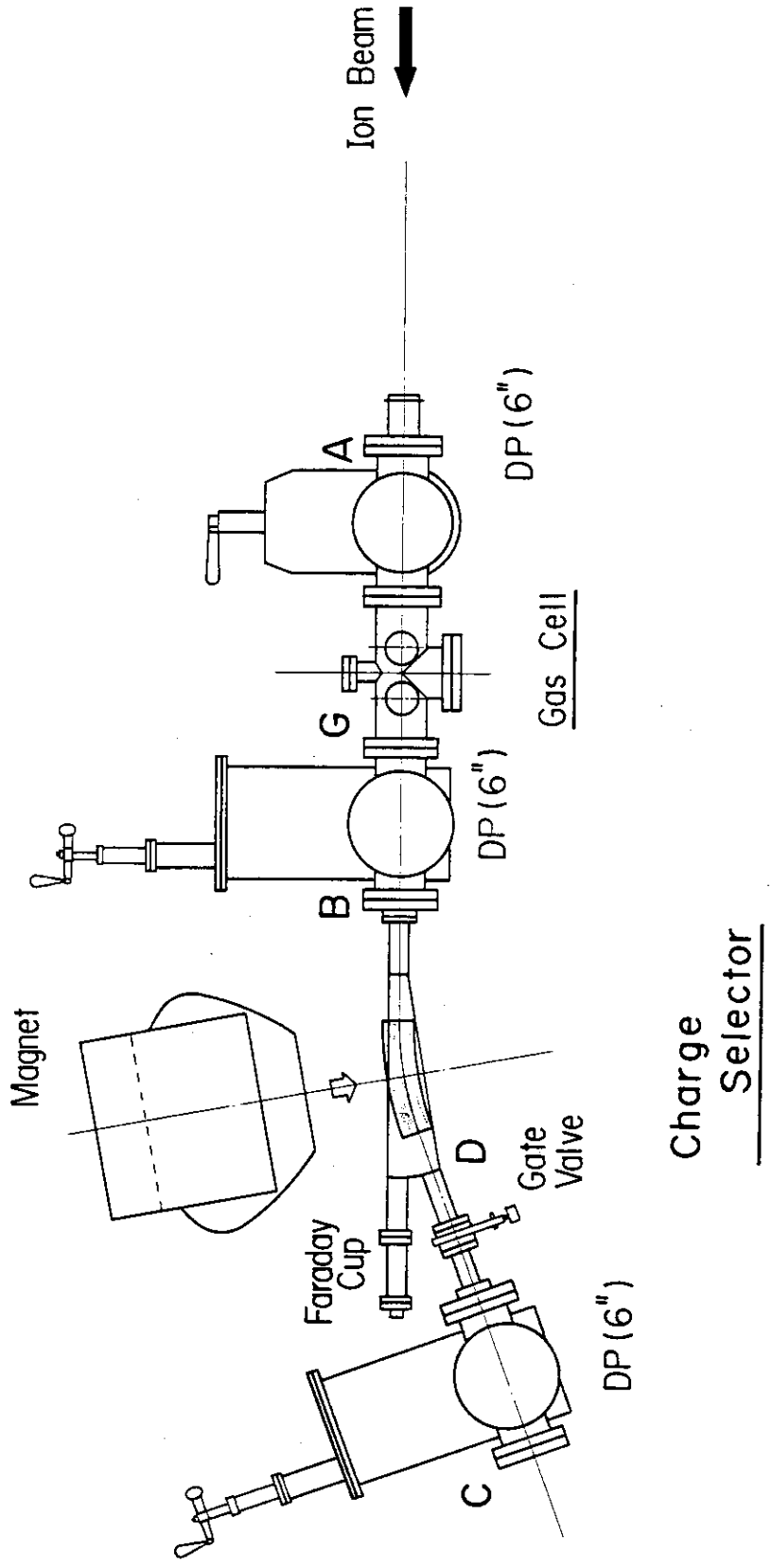

Fig.1.1 A Schematic diagram of the apparatus.

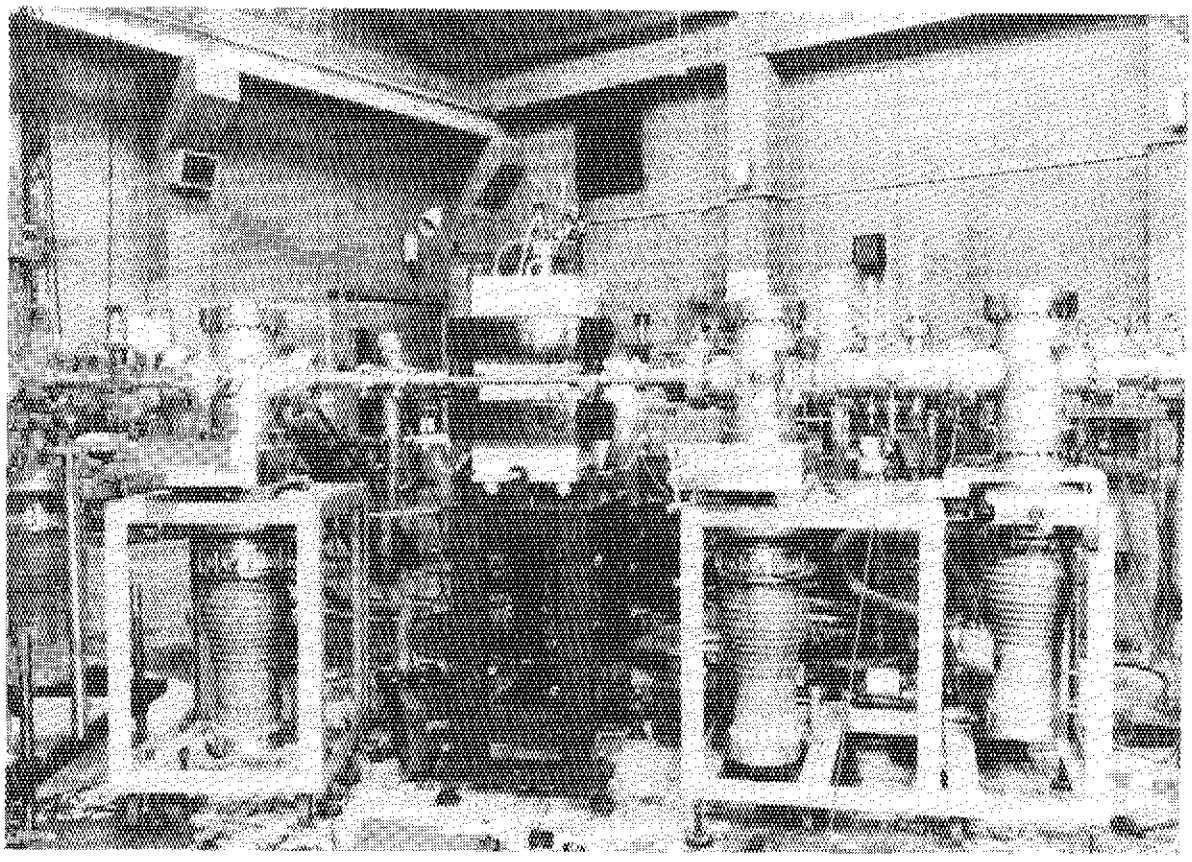

Fig.1.2 A photograph of the gas stripper cell

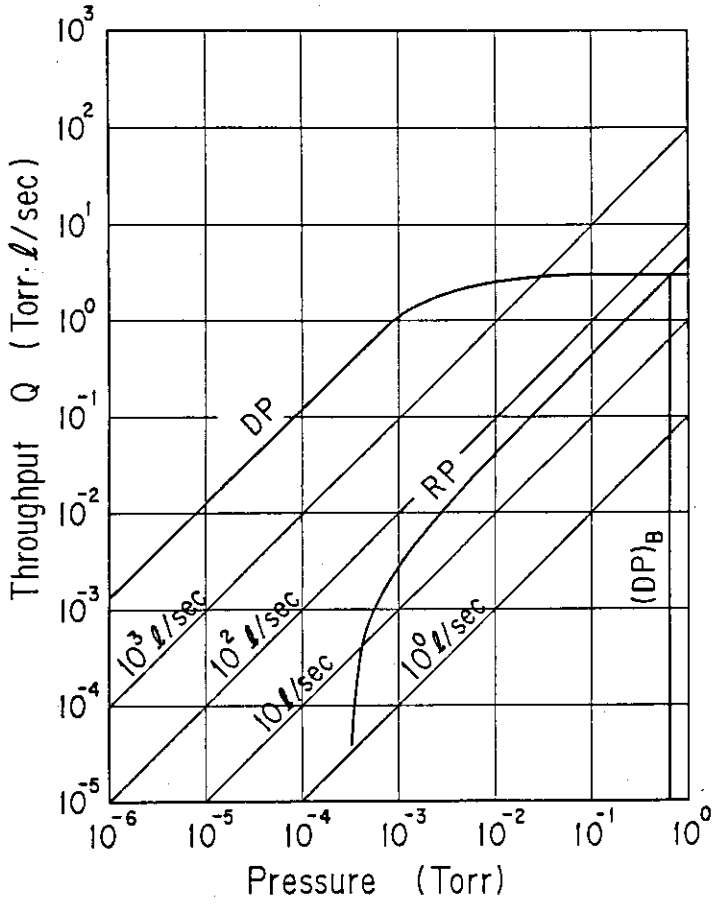

Fig.2.1 A Q-P diagram of the pumping system.

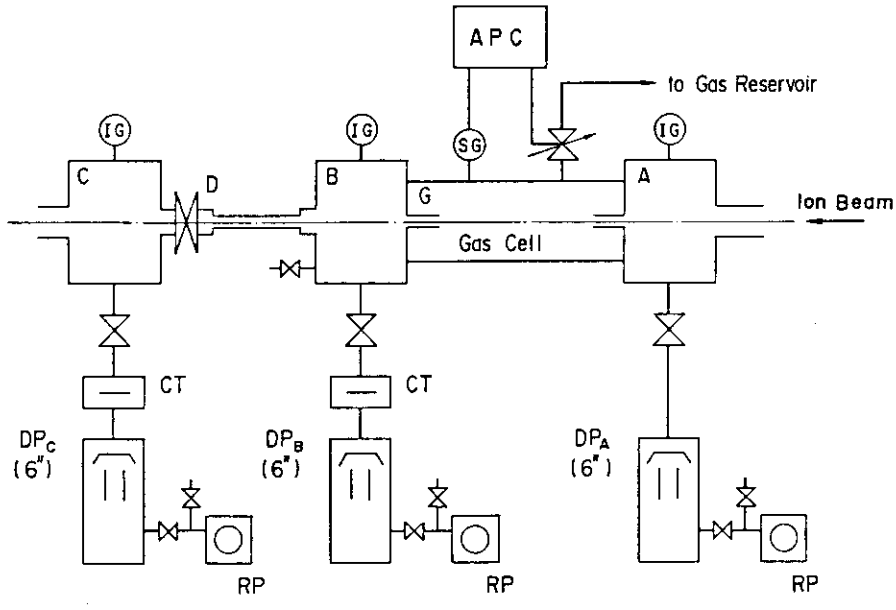

Fig.2.2 A Schematic diagram of the pumping system: IG; ion gauge, CT; cold trap, DP; diffusion pump, RP; rotary pump, APC; automatic pressure controller, SG; Schulz gauge.

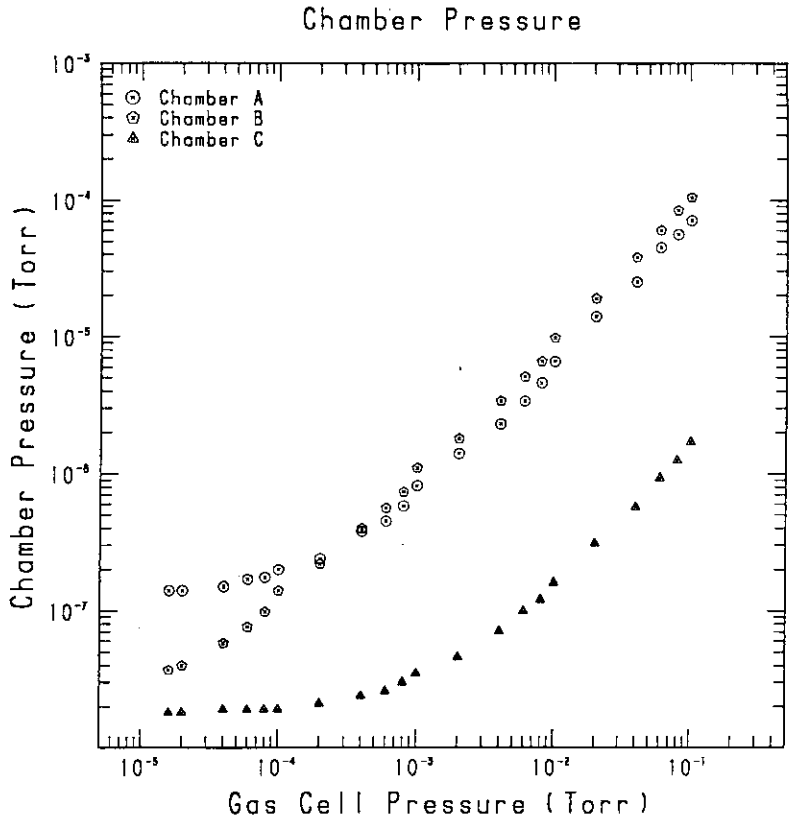

Fig.2.3 The gas pressure of chamber (A), (B) and (C), assigned in Fig. 2.2 as a function of gas cell pressure.

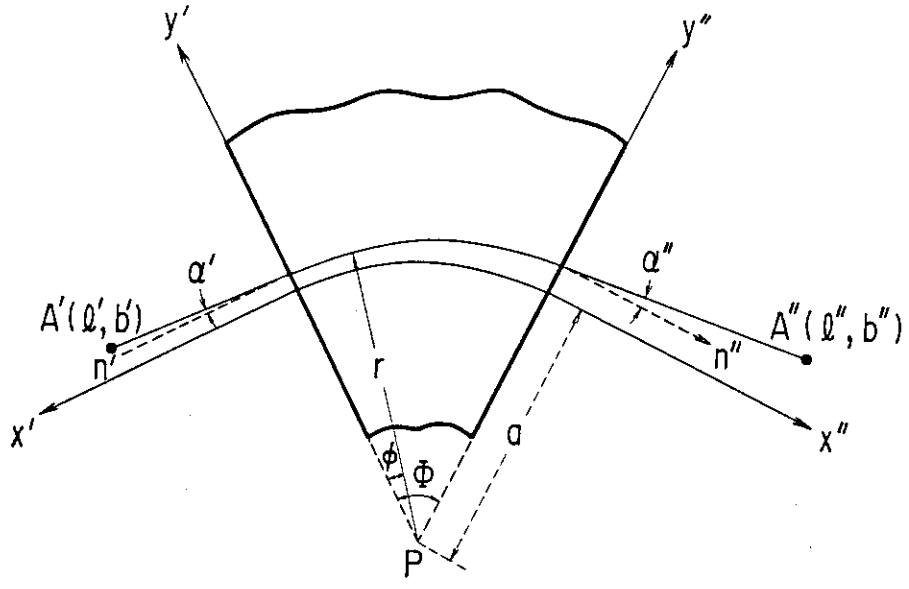

Fig.2.4 Diagram showing the ion orbit in the sector type magnet.

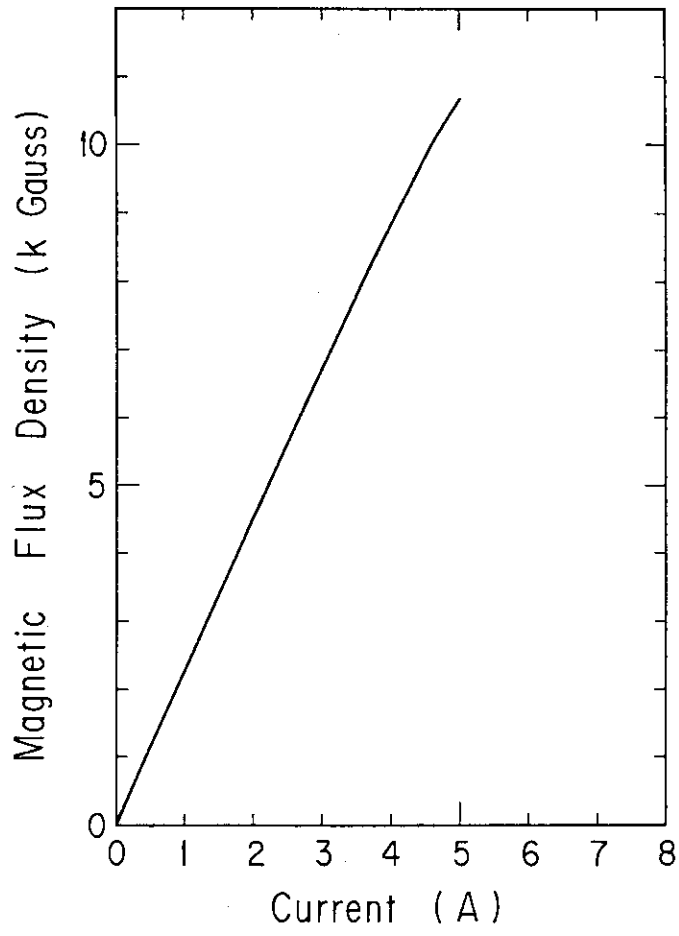

Fig.2.5 Calibration curve of the magnetic flux density of the magnet to the electric current through the magnetic coil.

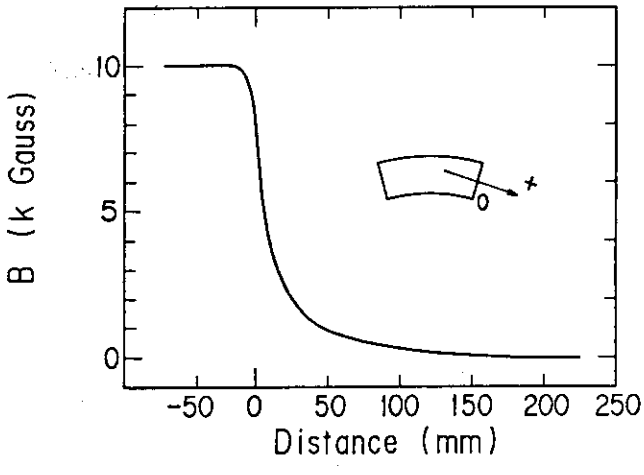

Fig.2.6 Magnetic field distribution parallel to the ion beam direction.

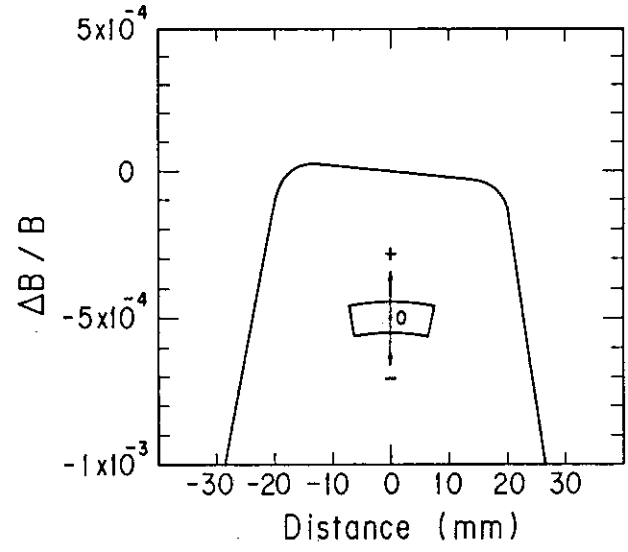

Fig.2.7 Magnetic field distribution perpendicular to the ion beam direction.

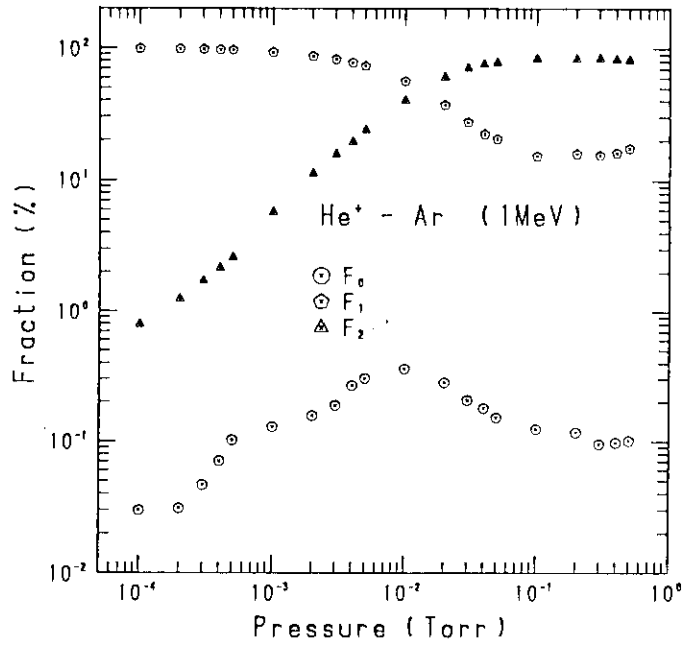

Fig.3.1 The pressure dependencies of the fractions of outgoing He^0, He^+ and He^{2+} beams (F_i) normalized by intensities of the outgoing ion beams at beam energy of 1.0 MeV.

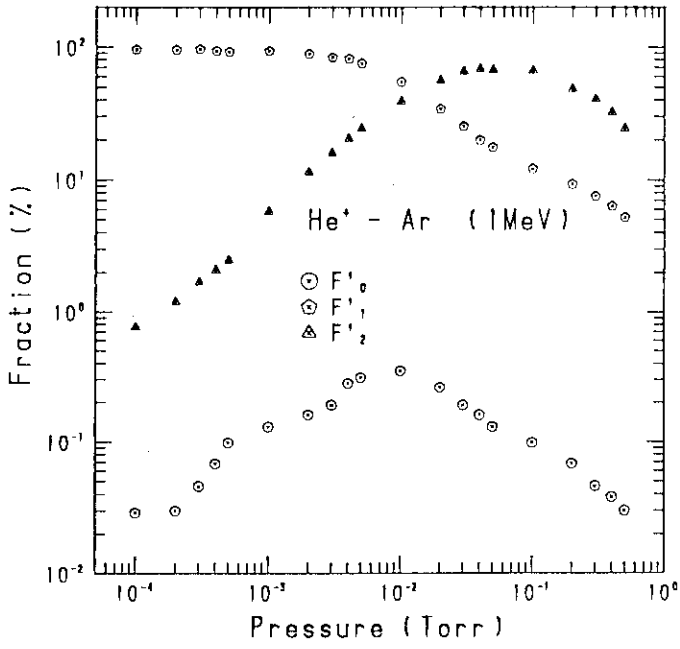

Fig.3.2 The pressure dependencies of the fractions of the outgoing He^0, He^+ and He^{2+} beams (F'_i) normalized by intensities of the incident ion beams at beam energy of 1.0 MeV.

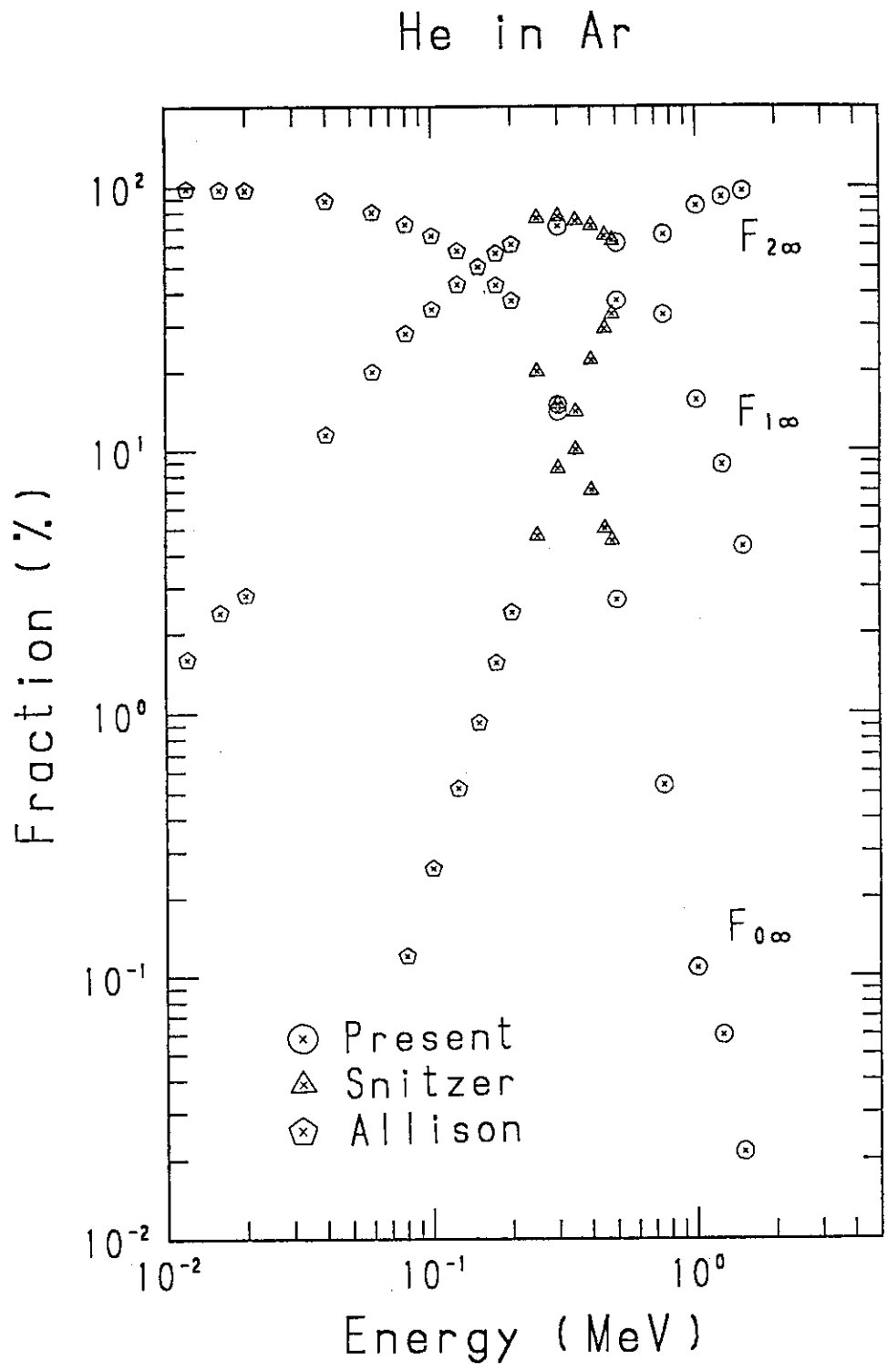

Fig.3.3 The equilibrium charge states fraction of He^{0}, He^{+} and He^{2+} beams ($F_{i\infty}$) in argon gas for the beam energy between 0.3 and 1.5 MeV.